

# ExMolRL: Phenotype–Target Joint Generation of De Novo Molecules via Multi-Objective Reinforcement Learning

Haotian Guo, Hui Liu\*

College of Computer and Information Engineering, Nanjing Tech University, Nanjing, 211800, China.  
hliu@njtech.edu.cn

## Abstract

The generation of high-quality candidate molecules remains a central challenge in AI-driven drug design. Current phenotype-based and target-based strategies each suffer limitations, either incurring high experimental costs or overlooking system-level cellular responses. To bridge this gap, we propose ExMolRL, a novel generative framework that synergistically integrates phenotypic and target-specific cues for de novo molecular generation. The phenotype-guided generator is first pretrained on expansive drug-induced transcriptional profiles and subsequently fine-tuned via multi-objective reinforcement learning (RL). Crucially, the reward function fuses docking affinity and drug-likeness scores, augmented with ranking loss, prior-likelihood regularization, and entropy maximization. The multi-objective RL steers the model toward chemotypes that are simultaneously potent, diverse, and aligned with the specified phenotypic effects. Extensive experiments demonstrate ExMolRL’s superior performance over state-of-the-art phenotype-based and target-based models across multiple well-characterized targets. Our generated molecules exhibit favorable drug-like properties, high target affinity, and inhibitory potency (IC50) against cancer cells. This unified framework showcases the synergistic potential of combining phenotype-guided and target-aware strategies, offering a more effective solution for de novo drug discovery.

## Introduction

In AI-driven drug design, generating high-quality candidate molecules remains a fundamental challenge (Sanchez-Lengeling and Aspuru-Guzik 2018; Pang et al. 2023). In recent years, deep generative models have made significant advances in molecular design (Gómez-Bombarelli et al. 2018; Aini et al. 2024; Brown et al. 2019). Most existing methods largely fall into two distinct paradigms: target-based and phenotype-based drug discovery. Target-based approaches mainly focus on well-characterized targets—such as receptors, enzymes and transport proteins (Hughes et al. 2011; Imming, Sinning, and Meyer 2006; Wishart et al. 2018)—and aim to design molecules that specifically bind to active sites or binding pockets. These methods leverage structural information to guide rational drug design and elucidate mechanisms of action. Nevertheless, their effectiveness relies heavily on the availability of accurate target struc-

tures and well-understood biological functions (Swinney and Anthony 2011; Polykovskiy et al. 2020; von Lilienfeld, Müller, and Tkatchenko 2020). In addition, target-based methods often overlook system-level cellular responses, limiting their ability to capture off-target effects and broader phenotypic consequences.

In contrast, phenotype-based strategies seek to identify bioactive compounds that elicit desired phenotypic changes in cellular systems (Vincent et al. 2022; Moffat, Rudolph, and Bailey 2014). This paradigm does not require prior knowledge of biological targets, allowing for a more holistic view of drug effects in complex cellular contexts. This is especially valuable when the underlying molecular mechanisms of a disease are poorly understood (Moffat et al. 2017; Meissner et al. 2022). However, large-scale experiments to observe drug-induced, system-level phenotypic effects remains prohibitively expensive and labor-intensive. (Swinney and Anthony 2011). Also, these experiments are difficult to standardize or automate, limiting the throughput of phenotype-based drug screening (Moffat et al. 2017). Fortunately, transcriptional profiles effectively capture how compounds perturb the cellular state, offering molecular-level readouts that reflect drug perturbations leading to higher-order phenotypes (Lamb et al. 2006). Due to their high throughput and cost-efficiency, gene expression signatures have been widely used to probe both genetic alterations and external stimuli that lie along the causal pathway between genotype and disease phenotype. In fact, differential expression signatures have been employed to identify compounds capable of inducing desired phenotypic shifts (Subramanian et al. 2017b). Accordingly, we use the terms “phenotypic profile” standing for the transcriptional profiles in this study.

To date, few efforts have leveraged the complementary strengths of target-based and phenotype-based paradigms. To bridge this gap, we propose ExMolRL, a generative framework that integrates phenotypic and target-specific information for de novo molecular generation. ExMolRL comprises two key components: 1) a phenotype-guided molecular generator trained on large-scale drug-induced phenotypic profiles enabling the conditional generation of molecules that elicit desired drug efficacy; and 2) a reinforcement learning module that fine-tunes the generator using docking-based affinity scores to guide optimization toward specific protein targets. To ensure robust and diverse molecu-

lar generation, we incorporate multiple designed regularization terms into RL objective, to mitigate reward exploitation and maintain molecular diversity and drug-likeness. Our extensive experiments demonstrate that ExMolRL can generate candidate molecules that simultaneously exhibit desired phenotypic effects, strong target affinity, and favorable drug-like properties. This unified framework showcases the synergistic potential of combining phenotype-driven and structure-aware strategies, offering a more comprehensive and effective solution for de novo drug discovery. Our main contributions are summarized as below:

- We propose a novel framework that integrates phenotypic profiles with target protein structures to jointly optimize molecular efficacy and specificity.
- We introduce ranking loss, prior likelihood, and entropy regularization to enhance stability, molecular diversity, and overall generation quality in reinforcement learning.
- Our method achieves superior performance over state-of-the-art phenotype-based and target-based models across multiple targets, simultaneously excelling in binding affinity, drug-likeness, and synthetic feasibility.

## Related Works

### Phenotype-Guided Molecular Generation

Phenotype-based molecular generation focuses on leveraging cellular-level response data—such as transcriptional profiles—to guide the design of compounds capable of modulating disease states (Vincent et al. 2022; Moffat, Rudolph, and Bailey 2014). This approach is particularly valuable for complex or poorly understood diseases where molecular mechanisms remain elusive. With the integration of deep learning and omics technologies, phenotype-driven drug discovery models have seen rapid development. For example, PacMann (Cadow et al. 2020) predicts drug sensitivity by modeling the relationship between gene expression profiles of cancer cell lines and compound SMILES representations, capturing phenotype-to-structure associations. TRIOMPHE (Kaitoh and Yamanishi 2021) employs a variational autoencoder conditioned on expression profiles to generate candidate molecules. Gex2SGen (Das et al. 2023) and GxVAEs (Li and Yamanishi 2024) followed similar ideas that used the desired expression profiles as input to design drug-like molecules capable of eliciting phenotypic changes. Mendez-Lucio et al. (Méndez-Lucio et al. 2020) further employed a generative adversarial network (GAN) in conjunction with expression profiles to automatically design molecules with a high probability to induce therapeutic effects. SmilesGEN (Liu, Tian, and Liu 2025) is a dual-channel variational autoencoder framework that jointly models drug molecules and gene expression profiles in a shared latent space to generate drug-like molecules capable of eliciting desired phenotypic effects.

### Target-based Molecular Design

Target-driven approaches make advantage of protein structure or binding pocket information to generate molecules with high binding affinity (Danel et al. 2023). For example, Pocket2Mol (Peng et al. 2022) constructs 3D point

clouds of binding pocket as conditional input and employs graph neural networks to generate molecular structures tailored to specific binding sites, which represents a typical docking-based generation paradigm. LiGAN (Méndez-Lucio et al. 2020) and AutoGrow4 (Spiegel and Durrant 2020) leverage the three-dimensional geometry of protein binding pockets together with fragment-assembly heuristics to generate molecules that satisfy spatial docking constraints. By contrast, OptiMol (Nigam et al. 2021) and SampleDock (Xu, Wauchope, and Frank 2021) employ a “generate–evaluate–select” workflow: they sample candidates from a learned latent space, score each via molecular docking, retain the highest-scoring compounds, and iteratively refine the generator based on this feedback. Moreover, SBMol-Gen (Ma et al. 2021) integrates reinforcement learning by treating docking scores as rewards, thereby steering the generative policy toward progressively more favorable chemotypes. Nevertheless, drug efficacy is governed by the intricate cellular environment, and molecules optimized exclusively for target binding frequently fail to produce the intended phenotypic outcomes.

## ExMolRL Framework

We present ExMolRL, a generative framework that integrates multi-modal data—including phenotypic profiles and chemical language—for the generation of drug-like molecules. ExMolRL comprises a phenotypic profile-guided generative module, and a reinforcement learning module that fine-tunes the agent toward desired molecular properties such as binding affinity and quantitative estimate of drug-likeness (QED) scores. The phenotypic generator is pre-trained on large-scale drug-induced expression profiles and then acts as prior model. Next, RL is utilized to refine the agent model toward desired molecular attributes, while mitigating reward hacking effects that may compromise molecular uniqueness. Once trained, ExMolRL generates molecules guided by expression profiles and informed by the structural context of target proteins.

### Phenotype-Guided Generator

The phenotype-guided generator aims to produce drug-like molecules conditioned on desired transcriptional profiles. Inspired by SmilesGEN (Liu, Tian, and Liu 2025), we adopt a dual-channel variational autoencoder (VAE) architecture, which consists of ExpVAE, a multi-layer feed-forward network used to encoding expression profiles, and MolVAE, a GRU-backed VAE designed to encode and reconstruct molecular SMILES sequences. MolVAE is firstly pre-trained on a large-scale SMILES dataset, after which its encoder is frozen. Next, joint training is performed using triplets comprising SMILES sequences, perturbed expression profiles, and corresponding unperturbed profiles. This allows for the simultaneous reconstruction of both molecular structures and expression profiles, leading to joint optimization of the parameters in ExpVAE and MolVAE.

The dual-VAE architecture learns a latent space that captures the complex relationship between phenotypic signatures and chemical structures, enhancing its capacity to generate biologically relevant molecules. During inference, we

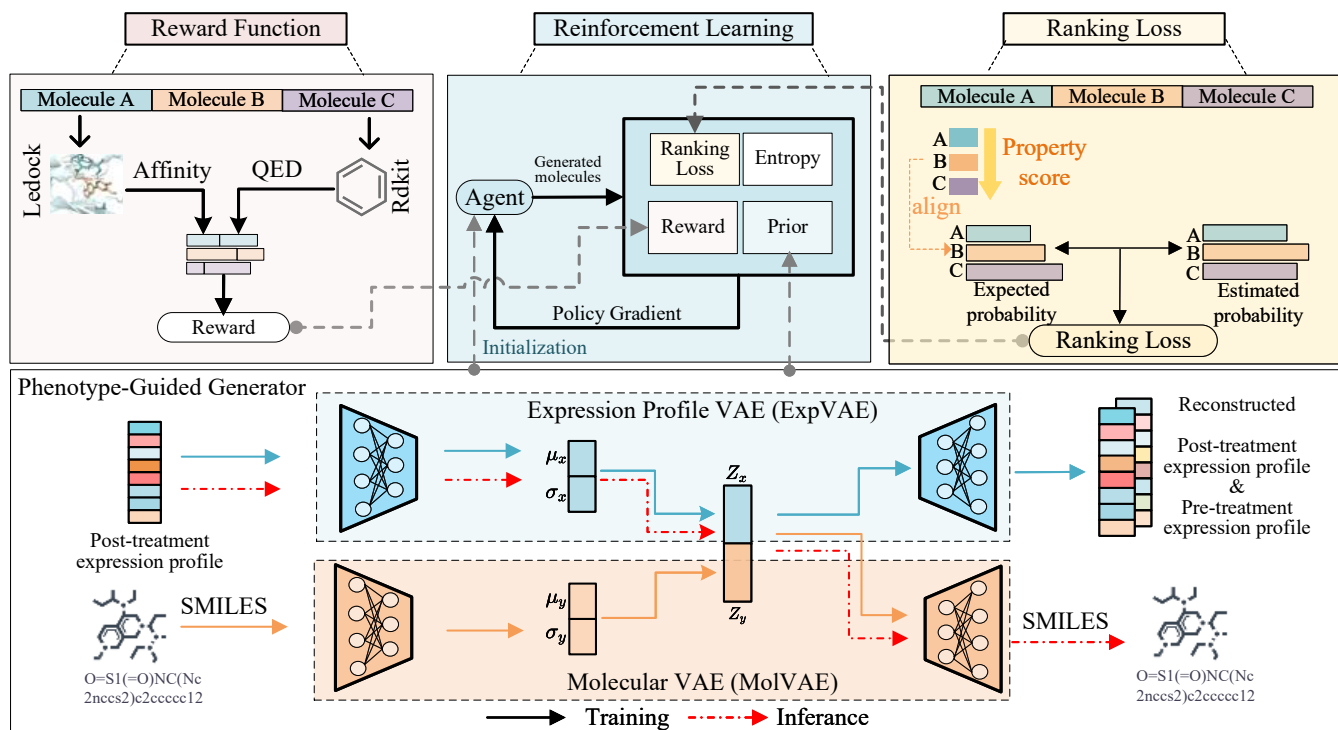


Figure 1: Overview of the ExMolRL architecture. The model consists of a pretrained phenotypic-profile-guided generator, while a reinforcement learning agent fine-tunes the molecular generation toward desired biochemical properties.

retain the encoder from ExpVAE and the decoder from MolVAE to enable phenotype-to-molecule generation. The trained generator serves as a prior model in the RL phase, constraining the policy to produce molecules aligned with desired phenotypic effect.

### Phenotype-Target Joint Generation

To jointly optimize phenotypic efficacy and target binding, we cast phenotype- and target-based molecular generation as a reinforcement learning (RL) problem. Specifically, the trained phenotypic generator serves as a prior, and an agent model adopts the same network architecture. During the RL phase, the agent is initialized with the prior’s parameters and optimized to maximize the task-specific reward function. Notably, the prior remains fixed throughout RL phase and serves as a regularizer, constraining the agent’s policy to generate molecules that induce biologically plausible phenotypic effects and preserving consistency with phenotype-conditioned distribution learned during pretraining.

To guide the generation of molecules with desirable properties, we incorporate both molecule-target docking scores and QED values into the reward function to encourage the agent to explore promising regions of the chemical space. The binding affinity between each generated molecule and its target protein is quantified using LeDock docking scores, a tool that has demonstrated strong performance in a recent benchmark study involving 2002 protein–ligand complexes (Zhao and Caflisch 2013; Wang et al. 2016). The QED score is computed using RDKit and incorporated into

the reward function. Let  $S = \{s_1, s_2, \dots, s_n\}$  denote a set of SMILES sequences, where each  $s \in S$  is of the form  $s = \{a_1, a_2, \dots, a_t\}$ , with  $a$  denoting a token in the sequence. For each SMILES sequence  $s$ , the reward function is defined as follows:

$$Reward(s) = Dock(s) \times QED(s) \quad (1)$$

where  $Dock$  denotes the normalized docking score and QED is the drug-likeness score of the generated molecule. A molecule is considered valid only if it satisfies RDKit’s validity check and its QED score exceeds a predefined threshold. If a generated molecule is deemed invalid (e.g., chemically implausible or syntactically incorrect), its docking score is set to zero as a form of penalty. Moreover, we have observed that imposing a mild constraint on QED scores helps guide the generation process toward molecules with a more favorable balance of properties, preventing the reward function from being dominated solely by docking scores or QED values. To normalize the docking score into the range  $[0,1]$ , we introduce a rescaling factor  $k$ , enabling better compatibility between different reward components. The full definition of the processed docking score is as follows:

$$Dock(s) = \begin{cases} \frac{\max(LeDock(s), k)}{k}, & \text{if } s \text{ is valid} \\ 0, & \text{otherwise} \end{cases} \quad (2)$$

The agent is trained to learn a policy  $\pi(\theta)$  that maximizes the reward expectation, where  $\theta$  represent the parameters of the agent model. Our approach builds upon the REINVENT

framework (Loeffler et al. 2024), which has been shown effective in molecular generation tasks, with modifications tailored to our task. To improve training efficiency and stabilize gradient estimation, we adopt a mini-batch training strategy. At each step, a batch of  $N$  molecules is sampled from the agent. For a SMILES sequence  $s$  generated from  $\pi_\theta$ , we compute its log-likelihood  $\log p^{(\text{agent})}(s)$  under the agent’s policy. We also obtain its prior log-likelihood  $\log p^{(\text{prior})}(s)$  by passing the same sequence into the prior model. The objective of RL is to maximize both the prior log-likelihood and reward. Accordingly, we adopt the policy gradient algorithm to maximize the objective and thus the loss function is defined as follows:

$$\mathcal{L}_{\text{pg}} = -\mathbb{E}_S[\log p^{(\text{agent})}(s; \theta) \cdot \text{Reward}(s)] \quad (3)$$

### Ranking Loss and Regularizers

Reinforcement learning in molecular generation often faces two key challenges: 1) sparse reward signals, which hinder effective policy learning, and 2) unstable sample quality, where the agent may exploit the reward function by generating low-quality yet high-reward molecules. To mitigate these issues and encourage the model to assign higher generation probabilities to molecules with superior properties (e.g., binding affinity, QED, or biological activity), we introduce a ranking loss constraint. Let the desired property score of a molecule be denoted as  $AS(s)$ , which is defined based on docking scores and relevant chemical properties. Given a pair of molecules  $(s_i, s_j)$  with  $AS(s_i) > AS(s_j)$ , we expect that the agent model assigns higher likelihood probability to the molecule with high property score. Specifically, the agent’s policy  $\pi$  is expected to satisfy the ranking constraint  $p^{(\text{agent})}(s_i|\pi(\theta)) > p^{(\text{agent})}(s_j|\pi(\theta))$  for all  $AS(s_i) > AS(s_j)$ . When a lower-quality molecule is assigned a higher generative probability than a higher-quality one, a ranking loss is incurred as below:

$$\mathcal{L}_{\text{rank}} = \sum_i \sum_{j>i} \max(0, f(s_j) - f(s_i) + \gamma_{ij}), \quad \forall i < j, AS(s_i) > AS(s_j) \quad (4)$$

where  $\gamma_{ij} = (j - i) \cdot \gamma$  is defined as the rank difference between two molecules multiplied by a hyperparameter  $\gamma$ . The function  $f(s)$  is defined as  $\log p^{(\text{agent})}(s; \theta)$ . By increasing the generative probability of high-quality molecules, RL no longer relies solely on sparse rewards, but instead incorporates fine-grained feedback through property-based ranking. This helps prevent the agent from overfitting to syntactically valid but chemically poor molecules. Compared to purely reward-driven optimization, the use of rank loss enables the model to effectively distinguish structurally similar molecules with significantly different properties, thereby enhancing its structural optimization capability.

To ensure the stability and effectiveness of RL, we introduce two additional regularizers: prior likelihood regularization (Gómez-Bombarelli et al. 2018; Loeffler et al. 2024) and entropy regularization (You et al. 2018; Zoph and Le 2016). To prevent the agent from deviating from the prior

model, we incorporate a prior likelihood term based on the phenotype-guided generator. This regularizer is defined as:

$$\mathcal{L}_{\text{prior}} = -\mathbb{E}_S[\log p^{(\text{prior})}(s)] \quad (5)$$

Here,  $\log p_{\text{prior}}(s)$  denotes the log-likelihood of a molecule  $s$  under the prior model. The prior poses the constraint that the generated molecules conform to valid SMILES syntax and chemically plausible structures, while also satisfying phenotype conditions with high fidelity. By imposing this prior constraint, the agent model benefits from the inductive biases encoded in the trained phenotypic generator, which improves its ability to respond accurately to phenotypic signatures. This is especially crucial in the early stages of RL, where the prior prevents the agent from cheating the reward function (“reward hacking”) by generating unrealistic or syntactically invalid molecules.

To encourage chemical space exploration and increase structural diversity, we introduce an entropy regularization term, which is defined as:

$$\mathcal{L}_{\text{ent}} = \mathbb{E}_S [H(s; \theta)] \quad (6)$$

in which  $H(s; \theta) = -\sum_{t=1}^T p(a|a_{<t}; \theta) \cdot \log p(a|a_{<t}; \theta)$  denotes the entropy of the agent’s action distribution over the next token. Maximizing this entropy encourages stochasticity in the policy, helping the agent avoid deterministic local optima and promoting molecular diversity.

Taking the ranking loss and two regularization terms into the policy gradient loss, the overall objective enable jointly optimize molecular quality while preserving generative capacity. The final loss function is defined as:

$$\mathcal{L} = \mathcal{L}_{\text{pg}} + \alpha \cdot \mathcal{L}_{\text{rank}} + \beta \cdot \mathcal{L}_{\text{prior}} - \lambda \cdot \mathcal{L}_{\text{ent}} \quad (7)$$

where  $\alpha$ ,  $\beta$ , and  $\lambda$  are hyperparameters used to tradeoff the weights of the ranking loss, prior and entropy regularization, respectively.

In our practice, we employed the bidirectional GRUs as the backbone of MolVAE. Both the encoder and decoder were composed of three hidden layers of size 192. The ExpVAE adopted multiple forward-feed layers with sizes 512, 256, and 192, respectively. During the training of phenotypic generator, the Adam optimizer is used with a learning rate of 5e-4 and a dropout rate of 0.1. The maximum length of the generated SMILES strings was restricted to 100 characters. In the RL stage, both agent model was optimized using Adam optimizer with a reduced learning rate of 1e-4. The batch size for both stages was set at 64. Our model was implemented using PyTorch 2.3.0. The training and all evaluation experiments were conducted on a CentOS Linux 8.2.2004 (Core) system, equipped with a GeForce RTX 4090 GPU and 128GB of memory.

## Experiments

### Datasets and Preprocessing

The MolVAE was pretrained using 10,032,879 SMILES sequences obtained from ZINC database (Irwin and Shoichet 2005), and then the ExpVAE and MolVAE were jointly trained using the L1000 dataset (Subramanian et al. 2017a),

	ExMolRL			SmilesGEN			GxVAEs			TRIOMPHE		
	Affinity	QED	SA	Affinity	QED	SA	Affinity	QED	SA	Affinity	QED	SA
AKT1	<b>-6.49</b>	<b>0.764</b>	<b>2.634</b>	-5.23	0.585	2.932	-5.77	0.583	3.207	-2.33	0.462	4.08
AKT2	<b>-6.34</b>	<b>0.729</b>	<b>2.844</b>	-5.84	0.610	3.06	-6.16	0.595	3.42	-2.95	0.445	4.25
AURKB	-6.71	<b>0.736</b>	<b>2.612</b>	-6.21	0.574	3.01	<b>-6.94</b>	0.599	3.276	-2.31	0.425	4.10
CTSK	-5.07	<b>0.675</b>	3.00	-4.81	0.604	<b>2.97</b>	<b>-5.33</b>	0.597	3.011	-1.87	0.399	4.47
HDAC1	<b>-4.64</b>	<b>0.729</b>	<b>3.197</b>	-3.51	0.566	3.017	-3.59	0.619	3.225	-1.84	0.437	4.30
MTOR	-6.27	<b>0.730</b>	<b>2.685</b>	-5.96	0.57	3.00	<b>-6.67</b>	0.605	3.324	-2.75	0.465	4.18
PIK3CA	<b>-6.04</b>	<b>0.731</b>	3.132	-5.65	0.578	<b>2.98</b>	-5.86	0.640	3.298	-2.88	0.435	4.50
SMAD3	<b>-5.16</b>	<b>0.676</b>	<b>3.212</b>	-3.54	0.577	3.01	-3.4	0.594	3.242	-2.57	0.464	4.15
TP53	<b>-7.01</b>	<b>0.755</b>	<b>2.81</b>	-4.56	0.593	2.97	-4.38	0.611	3.281	-2.64	0.417	4.17
EGFR	<b>-7.37</b>	<b>0.726</b>	<b>2.464</b>	-6.67	0.57	2.95	-7.33	0.58	3.58	-3.31	0.442	4.37

Table 1: Performance Comparison of ExMolRL versus Phenotype-Guided Methods on Affinity, QED and SA Metrics

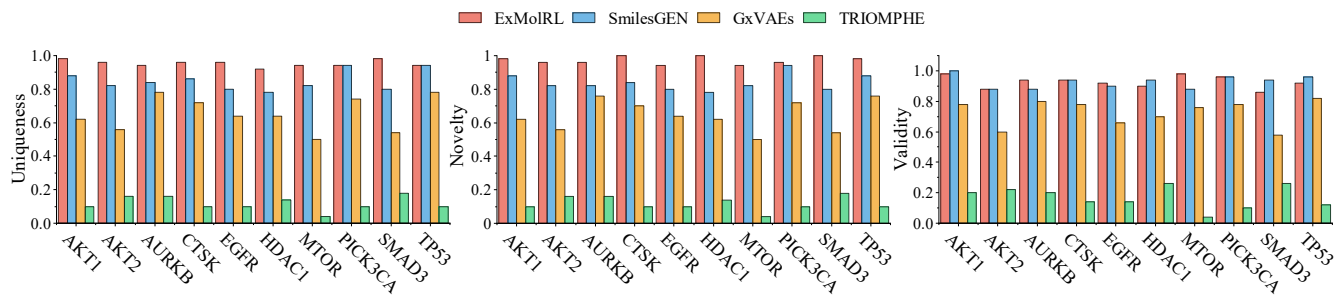


Figure 2: Performance Comparison of ExMolRL to Phenotype-Guided Methods on Uniqueness, Novelty and Validity

which was a collective repository of transcriptional responses of human cell lines to drug exposures. We extracted the expression profiles of cell lines treated by  $10\mu\text{M}$  drug concentration for 24 hours. To streamline the data, technical replicates were averaged. As a result, we obtained drug-induced expression profiles spanning 6,549 drugs and 164 cell lines. The refined dataset comprised a total of 86,400 expression profiles across 978 landmark genes to fine-tune the dual VAEs. In addition, to evaluate the binding affinity of generated molecules toward target proteins, we collected co-crystal structures of the ten protein–ligand complexes from the RCSB Protein Data Bank. Protein structures were pre-processed using the LePro tool (<http://www.lephar.com/>), and molecular docking was performed with the LeDock tool.

For performance evaluation, we used the expression profiles induced by the genetic perturbation of ten commonly target genes associated with the treatment of cancers. Among them, eight genes (AKT1, AKT2, AURKB, CTSK, EGFR, HDAC1, MTOR, and PIK3CA) were knockdown, and two genes (SMAD3 and TP53) were over-expressed. To evaluate the generated molecules, we obtained known ligands that have been confirmed to target these proteins from the Drug Target Commons (DTC) database (Tang et al. 2018). We compute the performance metrics between these known ligands and generated molecules.

## Performance Metrics

To evaluate the chemical properties of the generated molecules, we measured quite a few key metrics: validity, uniqueness, novelty, quantitative estimate of drug-likeness (QED), and synthetic accessibility (SA). High validity and uniqueness are indicators of an effective molecule generation process, while high novelty indicates the model avoids overfitting to the training set. For assessing binding affinity to target protein, we employed the docking scores computed by LeDock. In particular, we adopt  $\text{IC}_{50}$  as a key performance metric for evaluating phenotype-guided generative models.  $\text{IC}_{50}$  represents the concentration of a compound required to inhibit 50% of cancer cell viability, with lower values indicating greater inhibitory potency. In our experiments,  $\text{IC}_{50}$  values were predicted using the PaccMann platform (<https://ibm.biz/paccmann-aas>) (Cadow et al. 2020). These performance metrics ensures that our model was comprehensively evaluated in generating molecules with potential therapeutic value and practical feasibility.

## Comparison to Phenotype-Guided Methods

We first compare ExMolRL with several representative phenotype-based molecular generation methods, including SmilesGEN (Liu, Tian, and Liu 2025), GxVAEs (Li and Yamanishi 2024), and TRIOMPHE (Kaitoh and Yamanishi 2021). For each target protein, we generated 100 unique molecules using these methods and evaluated their performance across multiple metrics, as shown in Table 1. First,

	ExMolRL			Pocket2Mol			SampleDock			SBMolGen		
	Affinity	QED	SA	Affinity	QED	SA	Affinity	QED	SA	Affinity	QED	SA
AKT1	<b>-6.49</b>	<b>0.764</b>	2.634	-2.82	0.436	2.622	-4.70	0.749	<b>2.44</b>	-4.76	0.722	2.897
AKT2	<b>-6.34</b>	0.729	2.844	-5.99	0.612	3.362	-5.89	<b>0.751</b>	<b>2.17</b>	-5.49	0.710	3.042
AURKB	<b>-6.71</b>	0.736	2.612	-5.47	0.687	2.600	-4.74	0.685	<b>2.36</b>	-5.91	<b>0.737</b>	2.927
CTSK	<b>-5.07</b>	0.675	3.00	-4.67	0.723	2.803	-4.55	<b>0.789</b>	<b>2.276</b>	-4.61	0.713	3.032
HDAC1	<b>-4.64</b>	<b>0.729</b>	3.197	-2.35	0.507	2.535	-3.95	0.717	<b>2.197</b>	-3.54	0.713	2.95
MTOR	<b>-6.27</b>	0.730	2.685	-5.68	0.639	3.189	-5.54	<b>0.781</b>	<b>2.438</b>	-5.43	0.727	2.970
PIK3CA	<b>-6.04</b>	0.731	3.132	-4.70	<b>0.750</b>	2.826	-5.52	0.714	<b>2.552</b>	-5.53	0.706	2.936
SMAD3	<b>-5.16</b>	0.676	3.212	-3.72	0.598	<b>2.459</b>	-4.03	<b>0.778</b>	2.507	-3.92	0.747	3.091
TP53	<b>-7.01</b>	<b>0.755</b>	2.81	-5.25	0.656	3.351	-5.13	0.753	<b>2.439</b>	-5.51	0.709	2.992
EGFR	<b>-7.37</b>	0.726	<b>2.464</b>	-7.02	0.610	3.469	-6.18	0.705	2.465	-6.14	<b>0.737</b>	3.062

Table 2: Performance Comparison of ExMolRL versus Target-Based Methods on Affinity, QED and SA Metrics

ExMolRL achieved the best docking scores on 7 out of the 10 target proteins, with the generated molecules exhibiting significantly stronger binding affinities compared to those produced by SmilesGEN, GxVAEs, and TRIOMPHE. This highlights our model’s superior capability in optimizing chemical structure regarding specific binding pocket. Although GxVAEs performed comparably or slightly better on a few targets (e.g., AURKB and MTOR), its overall performance was inferior to our method, suggesting that our method offers better generalization and robustness across diverse protein contexts. Moreover, ExMolRL consistently achieved the highest QED scores across all ten target proteins, indicating that the generated molecules exhibit more drug-like pharmacological properties. Notably, even though SA scores were not explicitly included in the RL reward function, ExMolRL still outperformed the competing methods on most targets with respect to SA metric. We further analyzed the distribution of molecular property metrics across different methods. As shown in Figure S1, ExMolRL achieved substantially higher affinity than TRIOMPHE and SmilesGEN, with peaks concentrated in the high-affinity region (lower score means higher affinity). Meanwhile, ExMolRL consistently outperformed all competing methods in QED and SA score distributions, demonstrating its superior ability to generate drug-like and synthetically accessible compounds.

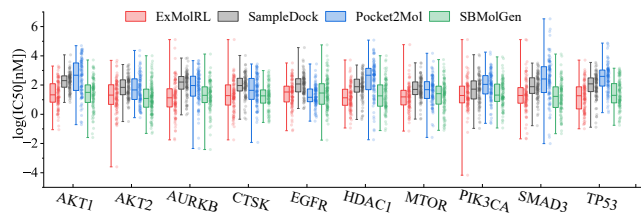


Figure 3: Performance comparison of ExMolRL versus targeted approaches in suppressing cancer cell viability

Moreover, we evaluated the uniqueness, novelty and validity of our generated molecules. As shown in Figure 2, ExMolRL outperformed four competing methods across all 10 targets, with novelty reaching 100% on targets such as TP53. These results demonstrate that ExMolRL consistently gen-

erates structurally novel compounds unseen during training.

### Comparison to Target-Based Methods

We next compared ExMolRL with three docking-based generative methods: Pocket2Mol (Peng et al. 2022), SampleDock (Xu, Wauchope, and Frank 2021), and SBMolGen (Ma et al. 2021). Similarly, we generated 100 unique molecules using each method for performance evaluation. As shown in Table 2, ExMolRL outperformed the competing methods in both docking scores and QED. Although SampleDock achieved slightly better SA scores, ExMolRL maintained competitive performance and consistently outperformed other baselines. We used EGFR as a representative target to analyze the distribution of evaluation metrics. As shown in Figure S2, ExMolRL exhibited substantial advantage over other methods in both docking and QED scores over competing methods, with peaks concentrated in the advantageous region. These results demonstrate that ExMolRL effectively leveraged both phenotypic guidance and target-specific docking signals, leading to superior molecular generation performance across multiple evaluation metrics.

Target-based methods focus solely on generating high-affinity molecules to specific target proteins, overlooking the effect on cellular contexts. In contrast, ExMolRL explicitly conditioned on the cellular state of the target protein to generate molecules that would induced desirable phenotypic profiles. To assess the effectiveness of this strategy, we further evaluated the ability of generated molecules to inhibit the viability of MCF7 breast cancer cells. Figure 3 showed the boxplots of the  $\log(\text{IC}_{50})$  values that measure the inhibitory potency of molecules generated by ExMolRL and competing methods across 10 target proteins. Note that lower  $\log(\text{IC}_{50})$  values indicate stronger inhibitory capacity. The results verified that ExMolRL consistently produced molecules with stronger anticancer potential across all targets compared to other methods. Moreover, the  $\text{IC}_{50}$  distributions of ExMolRL exhibited lower variance, indicating its stability to generate high-quality molecules. While SBMolGen did generate a few highly potent molecules with extremely low  $\log(\text{IC}_{50})$  values for specific targets such as AKT2 and SMAD, its overall distribution was broader and less stable. These results highlight that, compared to docking-based approaches, ExMolRL’s phenotypic gen-

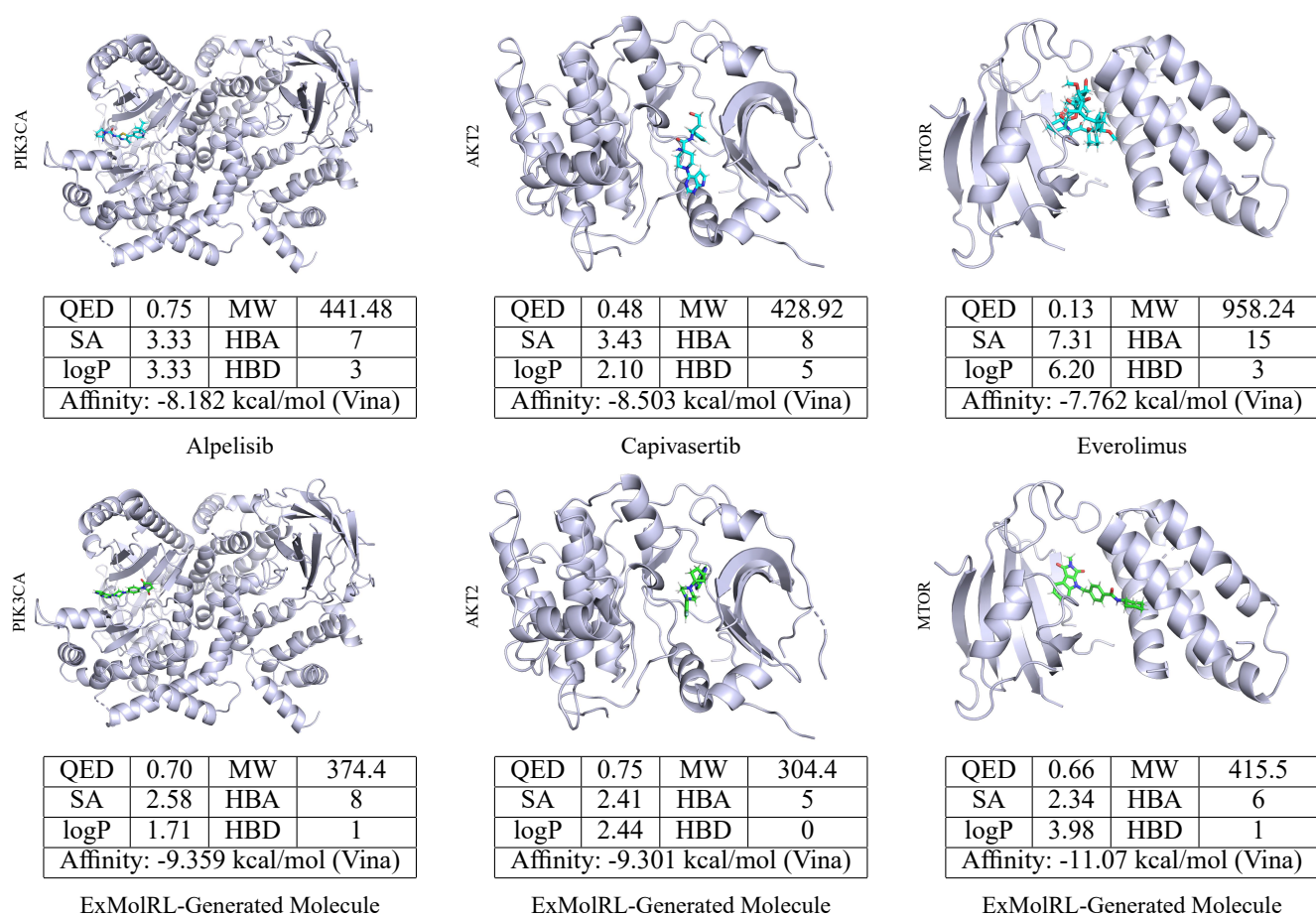


Figure 4: Comparison of ExMolRL-generated molecules versus approved drugs for the PIK3CA, AKT2, and mTOR targets.

conditioned strategy enables more effective and personalized molecule design, particularly for targeting cancer-specific cellular states.

### Therapeutic Molecular Generation

To assess ExMolRL’s ability to generate therapeutic compounds, we produced 100 novel molecules conditioned on breast cancer expression profiles and targeting PIK3CA, AKT2, and MTOR. These molecules were benchmarked against three FDA-approved drugs: Alpelisib (PI3K $\alpha$  inhibitor), Capiwasertib (AKT inhibitor), and Everolimus (mTOR inhibitor). All candidates were firstly filtered according to Lipinski’s Rule (LogP<5, MW<500Da, H-bond donors<5, H-bond acceptors<10), and then were docked to the target proteins using AutoDock Vina (Trott and Olson 2010). Other key physicochemical properties, including QED and synthetic accessibility (SA), were also computed for further evaluation. As shown in Figure 4, we illustrate the docking conformation of the three approved drugs (upper) and ExMolRL-generated candidates (bottom), alongside their QED, SA, and Vina scores. ExMolRL-generated molecules consistently outperformed the known drugs in binding affinity, achieving Vina scores

of  $-9.359$ ,  $-9.301$ , and  $-11.070$  kcal/mol versus  $-8.182$ ,  $-8.503$ , and  $-7.762$  kcal/mol for Alpelisib, Capiwasertib, and Everolimus, respectively. These candidates also exhibited improved drug-likeness and SA scores. Taking mTOR as example, Everolimus scored a QED of only 0.13 with an SA score of 7.31, whereas ExMolRL-generated candidate achieved a QED of 0.66 and an SA score of 2.34. Moreover, the generated candidate’s molecular weight (415.5 Da) and Log P align more closely with Lipinski criteria than Everolimus (958.2 Da), suggesting enhanced absorption and bioavailability. These results demonstrate that ExMolRL not only generates novel compounds with superior target binding, but also optimizes critical physicochemical properties.

### Conclusion

The proposed ExMolRL framework integrates phenotypic profiles and target protein structures via multi-objective reinforcement learning to generate de novo molecules with enhanced efficacy and specificity. Extensive experiments demonstrate its superiority over existing methods in drug-likeness, binding affinity, and phenotypic relevance, highlighting its potential for drug design.

## References

- Aini, N. S.; Ansori, A. N. M.; Herdiansyah, M. A.; Kharisma, V. D.; Widyandana, M. H.; Murtadlo, A. A. A.; Turista, D. D. R.; Sucipto, T. H.; Sahadewa, S.; Durry, F. D.; et al. 2024. Antimalarial Potential of Phytochemical Compounds from *Garcinia atroviridis* Griff ex. T. Anders Targeting Multiple Proteins of *Plasmodium falciparum* 3D7: An In Silico Approach. *BIO Integration*, 5(1): 967.
- Brown, N.; Fiscato, M.; Segler, M. H.; and Vaucher, A. C. 2019. GuacaMol: benchmarking models for de novo molecular design. *Journal of chemical information and modeling*, 59(3): 1096–1108.
- Cadow, J.; Born, J.; Manica, M.; Oskoei, A.; and Rodríguez Martínez, M. 2020. PaccMann: a web service for interpretable anticancer compound sensitivity prediction. *Nucleic acids research*, 48(W1): W502–W508.
- Danel, T.; Łęski, J.; Podlewska, S.; and Podolak, I. T. 2023. Docking-based generative approaches in the search for new drug candidates. *Drug Discovery Today*, 28(2): 103439.
- Das, D.; Chakrabarty, B.; Srinivasan, R.; and Roy, A. 2023. Gex2SGen: designing drug-like molecules from desired gene expression signatures. *Journal of Chemical Information and Modeling*, 63(7): 1882–1893.
- Gómez-Bombarelli, R.; Wei, J. N.; Duvenaud, D.; Hernández-Lobato, J. M.; Sánchez-Lengeling, B.; Sheberla, D.; Aguilera-Iparraguirre, J.; Hirzel, T. D.; Adams, R. P.; and Aspuru-Guzik, A. 2018. Automatic chemical design using a data-driven continuous representation of molecules. *ACS central science*, 4(2): 268–276.
- Hughes, J. P.; Rees, S.; Kalindjian, S. B.; and Philpott, K. L. 2011. Principles of early drug discovery. *British journal of pharmacology*, 162(6): 1239–1249.
- Imming, P.; Sinning, C.; and Meyer, A. 2006. Drugs, their targets and the nature and number of drug targets. *Nature reviews Drug discovery*, 5(10): 821–834.
- Irwin, J. J.; and Shoichet, B. K. 2005. ZINC- a free database of commercially available compounds for virtual screening. *Journal of chemical information and modeling*, 45(1): 177–182.
- Kaitoh, K.; and Yamanishi, Y. 2021. TRIOMPHE: transcriptome-based inference and generation of molecules with desired phenotypes by machine learning. *Journal of Chemical Information and Modeling*, 61(9): 4303–4320.
- Lamb, J.; Crawford, E. D.; Peck, D.; Modell, J. W.; Blat, I. C.; Wrobel, M. J.; Lerner, J.; Brunet, J.-P.; Subramanian, A.; Ross, K. N.; et al. 2006. The Connectivity Map: using gene-expression signatures to connect small molecules, genes, and disease. *science*, 313(5795): 1929–1935.
- Li, C.; and Yamanishi, Y. 2024. GxVAEs: Two Joint VAEs Generate Hit Molecules from Gene Expression Profiles. In *Proceedings of the AAAI Conference on Artificial Intelligence*, volume 38, 13455–13463.
- Liu, H.; Tian, S.; and Liu, X. 2025. Phenotypic Profile-Informed Generation of Drug-Like Molecules via Dual-Channel Variational Autoencoders. *arXiv preprint arXiv:2506.02051*.
- Loeffler, H. H.; He, J.; Tibo, A.; Janet, J. P.; Voronov, A.; Mervin, L. H.; and Engkvist, O. 2024. Reinvent 4: modern AI-driven generative molecule design. *Journal of Cheminformatics*, 16(1): 20.
- Ma, B.; Terayama, K.; Matsumoto, S.; Isaka, Y.; Sasakura, Y.; Iwata, H.; Araki, M.; and Okuno, Y. 2021. Structure-based de novo molecular generator combined with artificial intelligence and docking simulations. *Journal of Chemical Information and Modeling*, 61(7): 3304–3313.
- Meissner, F.; Geddes-McAlister, J.; Mann, M.; and Bantscheff, M. 2022. The emerging role of mass spectrometry-based proteomics in drug discovery. *Nature Reviews Drug Discovery*, 21(9): 637–654.
- Méndez-Lucio, O.; Baillif, B.; Clevert, D.-A.; Rouquié, D.; and Wichard, J. 2020. De novo generation of hit-like molecules from gene expression signatures using artificial intelligence. *Nature communications*, 11(1): 10.
- Moffat, J. G.; Rudolph, J.; and Bailey, D. 2014. Phenotypic screening in cancer drug discovery—past, present and future. *Nature reviews Drug discovery*, 13(8): 588–602.
- Moffat, J. G.; Vincent, F.; Lee, J. A.; Eder, J.; and Prunotto, M. 2017. Opportunities and challenges in phenotypic drug discovery: an industry perspective. *Nature reviews Drug discovery*, 16(8): 531–543.
- Nigam, A.; Pollice, R.; Krenn, M.; dos Passos Gomes, G.; and Aspuru-Guzik, A. 2021. Beyond generative models: superfast traversal, optimization, novelty, exploration and discovery (STONED) algorithm for molecules using SELFIES. *Chemical science*, 12(20): 7079–7090.
- Pang, C.; Qiao, J.; Zeng, X.; Zou, Q.; and Wei, L. 2023. Deep generative models in de novo drug molecule generation. *Journal of Chemical Information and Modeling*, 64(7): 2174–2194.
- Peng, X.; Luo, S.; Guan, J.; Xie, Q.; Peng, J.; and Ma, J. 2022. Pocket2Mol: Efficient Molecular Sampling Based on 3D Protein Pockets. In *International Conference on Machine Learning*.
- Polykovskiy, D.; Zhebrak, A.; Sanchez-Lengeling, B.; Golovanov, S.; Tatanov, O.; Belyaev, S.; Kurbanov, R.; Artamonov, A.; Aladinskiy, V.; Veselov, M.; et al. 2020. Molecular sets (MOSES): a benchmarking platform for molecular generation models. *Frontiers in pharmacology*, 11: 565644.
- Sanchez-Lengeling, B.; and Aspuru-Guzik, A. 2018. Inverse molecular design using machine learning: Generative models for matter engineering. *Science*, 361(6400): 360–365.
- Spiegel, J. O.; and Durrant, J. D. 2020. AutoGrow4: an open-source genetic algorithm for de novo drug design and lead optimization. *Journal of cheminformatics*, 12(1): 25.
- Subramanian, A.; Narayan, R.; Corsello, S. M.; and et al. 2017a. A Next Generation Connectivity Map: L1000 Platform and the First 1,000,000 Profiles. *Cell*, 171(6): 1437–1452.e17.
- Subramanian, A.; Narayan, R.; Corsello, S. M.; et al. 2017b. A Next Generation Connectivity Map: L1000 Platform and the First 1,000,000 Profiles. *Cell*, 171(6): 1437–1452.e17.

Swinney, D. C.; and Anthony, J. 2011. How were new medicines discovered? *Nature reviews Drug discovery*, 10(7): 507–519.

Tang, J.; Ravikumar, B.; Alam, Z.; Rebane, A.; Vähä-Koskela, M.; Peddinti, G.; van Adrichem, A. J.; Wakkinen, J.; Jaiswal, A.; Karjalainen, E.; et al. 2018. Drug target commons: a community effort to build a consensus knowledge base for drug-target interactions. *Cell chemical biology*, 25(2): 224–229.

Trott, O.; and Olson, A. J. 2010. AutoDock Vina: improving the speed and accuracy of docking with a new scoring function, efficient optimization, and multithreading. *Journal of computational chemistry*, 31(2): 455–461.

Vincent, F.; Nueda, A.; Lee, J.; Schenone, M.; Prunotto, M.; and Mercola, M. 2022. Phenotypic drug discovery: recent successes, lessons learned and new directions. *Nature Reviews Drug Discovery*, 21(12): 899–914.

von Lilienfeld, O. A.; Müller, K.-R.; and Tkatchenko, A. 2020. Exploring chemical compound space with quantum-based machine learning. *Nature Reviews Chemistry*, 4(7): 347–358.

Wang, Z.; Sun, H.; Yao, X.; Li, D.; Xu, L.; Li, Y.; Tian, S.; and Hou, T. 2016. Comprehensive evaluation of ten docking programs on a diverse set of protein–ligand complexes: the prediction accuracy of sampling power and scoring power. *Physical Chemistry Chemical Physics*, 18(18): 12964–12975.

Wishart, D. S.; Feunang, Y. D.; Guo, A. C.; Lo, E. J.; Marcu, A.; Grant, J. R.; Sajed, T.; Johnson, D.; Li, C.; Sayeeda, Z.; et al. 2018. DrugBank 5.0: a major update to the DrugBank database for 2018. *Nucleic acids research*, 46(D1): D1074–D1082.

Xu, Z.; Wauchope, O. R.; and Frank, A. T. 2021. Navigating chemical space by interfacing generative artificial intelligence and molecular docking. *Journal of Chemical Information and Modeling*, 61(11): 5589–5600.

You, J.; Liu, B.; Ying, Z.; Pande, V.; and Leskovec, J. 2018. Graph convolutional policy network for goal-directed molecular graph generation. *Advances in neural information processing systems*, 31.

Zhao, H.; and Caffisch, A. 2013. Discovery of ZAP70 inhibitors by high-throughput docking into a conformation of its kinase domain generated by molecular dynamics. *Bioorganic & medicinal chemistry letters*, 23(20): 5721–5726.

Zoph, B.; and Le, Q. V. 2016. Neural architecture search with reinforcement learning. *arXiv preprint arXiv:1611.01578*.